Wettability of cokes by Fe-Mn melt

Hamideh Kaffash, Xing Xing & Merete Tangstad

Published online: 07 Jan 2020.

Submit your article to this journal 🗗

Article views: 242

View related articles 🗗

View Crossmark data 🗗

Taylor & Francis
Taylor & Francis Group

🔓 OPEN ACCESS | Check for updates

# Wettability of cokes by Fe-Mn melt

Hamideh Kaffash[a] 🔘, Xing Xing[b], and Merete Tangstad[a]

[a]Department of Materials Science and Engineering, Norwegian University of Science and Technology, Trondheim, Norway; [b]School of Material Science and Engineering, University of New South Wales, Sydney, Australia

ABSTRACT
Four metallurgical cokes were heat treated at 1250 °C to 1550 °C in argon atmosphere. The influence of heat treatment on the microstructure of metallurgical cokes was characterized using X-ray diffraction and Raman spectroscopy. Wettability experiments were carried out using the sessile drop technique. The wettability of cokes with liquid Fe-85wt%Mn at 1550 °C was measured as a function of time. The effect of coke ash content, microstructure, porosity and roughness on the wettability was investigated. In the process of heat treatment, the microstructure of the metallurgical cokes transformed toward the graphitic structure. The Raman spectra showed variations reflecting their temperature histories. Area fraction of G peak increased as the annealing temperature increased and intensity ratios of D to G band decreased with temperature. All the four coke samples showed non-wetting behavior with Fe-85wt%Mn while graphite showed wetting behavior. Coke E with the highest roughness and porosity showed the lowest wettability compared to other cokes. Crystallite size of the coke samples did not seem to have any significant effect on the wettability.

GRAPHICAL ABSTRACT
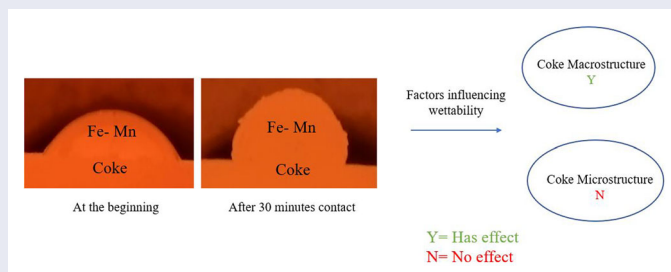
HIGHLIGHTS

- Fe-85wt%Mn does not wet cokes while it wets graphite
- Cokes with higher porosity and surface roughness showed lower wettability with Fe-85wt%Mn
- Coke graphitization degree, did not affect the wettability between cokes and Fe-85wt%Mn

Introduction

In Ferromanganese production, the carbon which is fed from top of the furnace is mostly consumed through reduction of metal oxides. But some of carbon is also dissolved into the metal up to saturation level.[1] The interaction of metal and carbon is important, because a large part of the dissolution reactions takes place between liquid metal and solid carbon in the form of coke, charcoal etc. Since mass transfer and heat transfer are the basic reactions involved in process, wetting is, therefore, the first step toward carbon dissolution.

A great deal of work has been performed in recent years by the group of Sahajwalla to characterize the wettability of reductants in iron-based hot metal. It was found that forming an ash layer between iron and coke would reduce the wettability and hence dissolution rate.[2,3] All of these results are based on wettability of iron-based hot metal, sometimes with controlled sulfur and carbon additions.[2,4] Some studies confirmed that sulfur content in the coke would retard the wettability by blocking the surface and reducing the contact surface between substrate and metal.[2] Rahman[5] found that sulfur content in coke would retard the surface tension between slag and coke and consequently decreased the

Table 1. Proximate analysis of carbon materials.

Property (unit)	Coke C	Coke D	Coke E	Coke F	Graphite
Fix C(pct)	85.28	89.34	85.57	87.93	98.6
Ash (wt pct)	11.82	9.61	13.68	11.42	0.3
VM (wt pct)	1.43	1.05	1.35	1.15	0.8

Table 2. Ash analysis of cokes.

Carbonaceous material	Ash(%db)							
	SiO_2	Al_2O_3	Fe_2O_3	CaO	MgO	MnO	K_2O	S
Coke C	6.97	3.07	0.87	0.66	0.24	0.08	0.03	0.44
Coke D	4.22	2.84	0.83	0.42	0.19	0.1	0.22	0.50
Coke E	7.35	3.96	0.95	0.43	0.09	0.01	0.11	0.63
Coke F	6.29	2.87	0.68	0.39	0.18	0.01	0.23	0.50
Graphite*	–	–	–	–	–	–	–	–

*Total ash content of the graphite is 0.3%. Ash composition analysis has not been conducted for graphite.

wettability. Some researchers[6–8] studied the effect of surface active elements in liquid Fe on wettability. It was found that the presence of surface active elements such as S and O alters the energy at the interface and hence the contact angle.

Microstructure of carbonaceous materials has been extensively studied using x-ray diffraction (XRD) and Raman spectroscopy.[9–13] Heating of cokes was shown to have a significant impact on the growth of crystallite size, L_c, by demonstrating the correlation between crystallite size and annealing temperature.[9,10] Correspondingly, the proportion of graphite-like structure increased during the thermal heating process.[10,11] It was also reported that crystallinity of the carbon materials would not have significant effect on their wettability with iron.[4]

Contradictory observations have been reported in the literature on the effect of carbon porosity on dissolution rate. Deng et al.[14] in the literature review of the paper mentioned that coke with lower porosity has a higher rate of dissolution. On the contrary, Mourao et al.[15] reported that coke with high porosity exhibit higher dissolution and further suggested that higher porosity offers more surface area for reaction and its effect seems to be more significant in the initial period of dissolution. Depending on the hydrodynamic condition of the bath, liquid metal penetrates the pores and thus, a larger surface area will participate in the reaction. At the later stage, the liquid metal may be trapped in the pores and tend to get saturated by carbon. This will make the inner surface area relatively ineffective.

Wettability between carbon materials (graphitic and non-graphitic) and iron has been reported in different literatures.[3,16] It was found in mentioned literatures that the ash layer between non-graphitic carbon materials and iron could be directly responsible for the decrease in wettability.

It is well accepted that wetting phenomena occurring on flat, rough surfaces are quite different.[17,18] Most practical solid surfaces are rough to some extent. The relationship between roughness and wettability was defined by Wenzel[19] who derived a simple relation based on the consideration of the effect of change in surface energy due to different surface roughness. If it is assumed that true surface area is α_T and apparent area is α_A, then usually $\alpha_T > \alpha_A$ without gas trapped in interface:

$$\cos\theta_R = R \cos\theta_S \quad (1)$$

Here R ($R \geq 1$) is the roughness factor, defined as α_T/α_A. θ_R and θ_s are contact angles on rough surface and smooth surface, respectively. His theory was based on the assumption that a rough surface extends the solid-liquid interface area in comparison to the projected smooth surface. This simple model has been found to be useful in capturing experimentally observed influence on the contact angle for simple roughness topography and for well wetting surface where the practical range of the contact angle, θ, is $0° < \theta < 90°$. The more complex case is that where the contact angle lies in the range $90° < \theta < 180°$. In this case, liquid does not penetrate well the rough surface asperities, and gas molecules can be trapped in the asperity valleys and the Wenzel model does not apply. In this case the Cassie-Baxter model is used instead. According to this model, air can remain trapped below the drop, forming air pockets. Thus non-wetting behavior is strengthened because the drop sits partially on the air. Cassie Baxter model[20] is shown as Equation (2) where φ is the area fractions of solid and air under a drop on the substrate. θ_R and θ_S are contact angles on rough surface and smooth surface, respectively. This equation simply indicates the contact angle can be increased even when the intrinsic contact angle of a liquid on the original smooth surface is less than 90°. In particular range of the surface roughness and hydrophobicity the Cassie-Baxter and Wenzel states could coexists.[21]

$$\cos\theta_R = \varphi(\cos\theta_S + 1) - 1 \quad (2)$$

Ciftja[22] studied the wetting behavior of molten silicon with graphite materials with different surface roughness. Here the graphite will be transformed to SiC at the surface. When the surface is smooth (Ra $< 0.1 \mu m$), the final contact angle for all the graphites is about 30°. As the surface becomes rougher, the final contact angle decreases, and it can reach even zero. In that case the silicon is absorbed completely by the graphite materials.

The aim of this paper is to study the wetting behavior of different metallurgical cokes by liquid Mn-ferroalloy at 1550 °C. Factors influencing wettability such as microstructure, surface roughness and porosity of carbon materials, were investigated.

Experimental

Four metallurgical cokes which was supplied by industry, cokes C, D, E and F, were studied in this work. Synthetic graphite was also studied as a reference material. Proximate analysis and ash composition of cokes are shown in Tables 1 and 2, respectively.

For sessile drop experiments, all carbon materials as substrates were cut in tablets with 10 mm diameter and 2–3 mm height. A small cylinder was cut from the alloy (Fe-85 wt%Mn) and used as metal droplet in sessile drop experiments. The reason that this alloy was chosen for the wetting studies is that in Electric Arc Furnace, the produced metal will contain high amount of manganese. If we take high manganese slag practice, 74–82% manganese would be in the metal.[23] If we
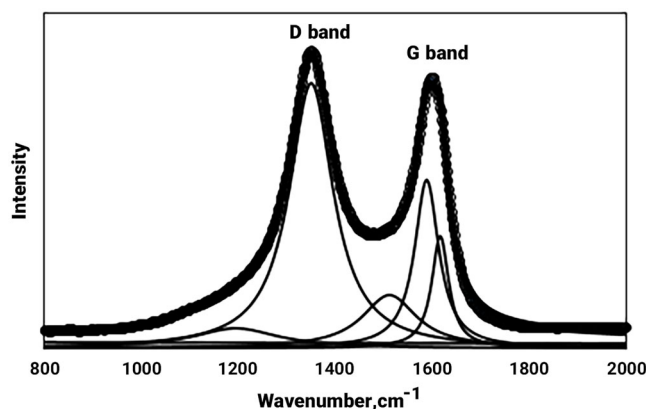
Figure 1. Typical Raman profile for metallurgical coke F annealed at 1450 °C.

Figure 2. Schematic diagram of the sessile drop furnace used for wetting experiments.

discard slag practice, 85–90% manganese would be in the metal.[24] We chose a manganese percentage between these two values to more or less evaluate both options

Three lumps of each coke with particle size of 19–22 mm were heat treated at 1250 °C, 1450 °C and 1550 °C for 30 minutes under the argon atmosphere in a resistance furnace. The samples were contained in a graphite crucible, into which 2.5 dm³/min of argon gas (99.9% pct) was continuously blown. The furnace temperature was increased to 400 °C with the rate of 25 °C min⁻¹ and then held for one minute before further increased to the target temperatures with the same heating rate. A B-type thermocouple connected with a PID temperature controller was used to control the furnace temperature, the temperature of samples during experiments was determined using a C-type thermocouple inserted into the graphite crucible.

The X-ray diffraction profile of coke samples was collected using Philips X'Pert multipurpose X-ray diffraction system (MPD). The wavelength of incident X-ray for Cu Ka radiation in this study was 1.5409 Å. Powdered coke samples were scanned in the range of 2θ from 10 to 50° with a step of 0.02°. The crystallite size, L_c, or stack height and interlayer spacing between aromatic planes of carbon crystallites, d_{002} were calculated using the Scherrer equation and Bragg's Law.

Carbonaceous materials were also analyzed using a Renishaw in Via Raman microscope with a 523 nm excitation wavelength. The beam size was 1.5 to 2 μm. Raman spectra were scanned from 800 to 2000 cm⁻¹ with 25 mW laser power for an exposure time of 15 seconds. At least ten measurements in different zones were taken for each sample.

Raman spectra of coke has two peaks around 1360 cm⁻¹ and 1580 cm⁻¹. The former and the latter peaks are known as D band and G band, respectively. D band is originating from defect structure of graphite and G band is related to normal graphite structure. In general, intensity ratios of these two bands I_D/I_G are used to evaluate an imperfection of carbon structure, where I_D is D band intensity and I_G is G band. In the present work, overlapped G and D bands were deconvoluted into five peaks with Lorentzian band fitting. Figure 1 shows a typical first order Raman profile of a metallurgical coke annealed at high temperature. The G fraction which characterizes coke graphitization was calculated as ratio of area under the G peak to the total area.[10]
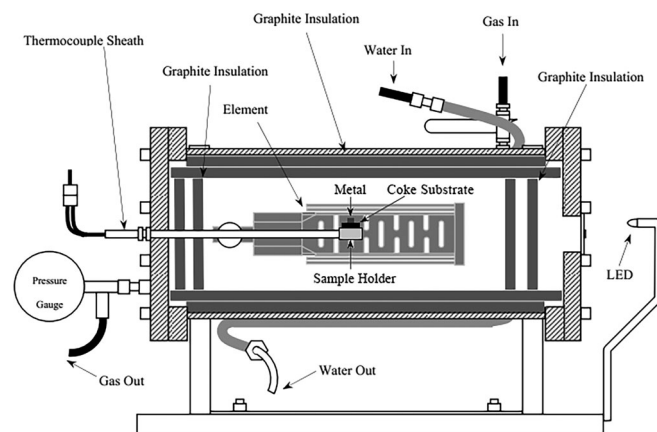
Keyence VK-X250 Laser Microscope was used to measure the surface roughness of carbon materials. The laser system can create three-dimensional surface images. For measuring the porosity of the carbon materials, a caliper was used to measure the volume of the carbon substrate (disc shape) and with having the mass of the substrate, the apparent density was calculated. The absolute density was determined using a Micromeritics Accupyc II 1340 Helium Pycnometer.

The wettability of cokes with Fe-85wt%Mn was determined in a graphite furnace shown in Figure 2. The furnace was designed with high cooling rate which allowed the samples to be quenched to the temperature below the melting point quickly after experiments. The metal/carbon assembly were placed on a graphite stage and slide in the hot zone of the furnace. Weights of the substrate (∼0.2 g) and metal (∼0.37 g) were recorded prior to experiment. The furnace chamber was evacuated initially, and then backfilled with the Ar with a flow rate of 1.5 NL/min (normal liter) until the end of the test. The temperature increased with the heating rate 25 °C/min to 1550 °C and then kept for 30 minutes to make the isothermal condition. The melting of metal marked the beginning of contact time. A Sony DCR-TRV18E digital video camera was used to record image sequences during the wettability experiments. This camera gives images at a resolution of 720 × 576 pixels. A pair of Vivitar zoom lenses (one 4×, one 1×) are screwed onto the camera lens to provide the correct focal length for viewing within the furnace. ImageJ software was used to determine the contact angle by an average of the two sides as the difference is within acceptable limits for the method used.

A scanning electron microscope (SEM), Hitachi S-3400, accompanied with Energy Dispersive Spectrometer was used to study the interface between coke and metal after sessile drop experiment.

Results and discussion

Wetting results

The contact angle between metal and coke substrate versus time and temperature is shown in Figure 3. It can be seen
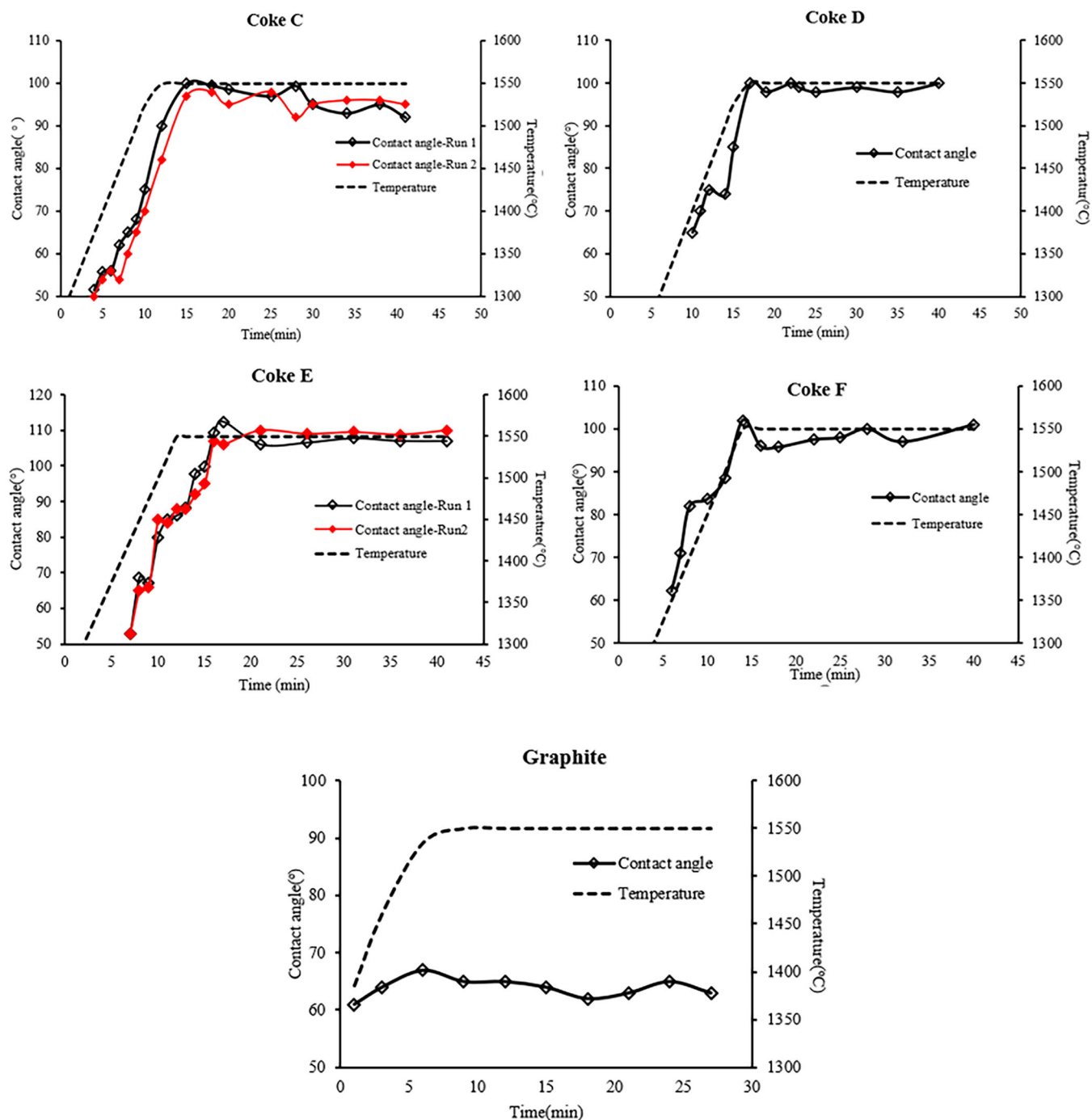
**Figure 3.** Contact angle versus time and temperature for cokes and graphite with liquid Fe-85wt%Mn.

from Figure 3 that the contact angles for all cokes and graphite were between 60 and 70° when metal started to melt (around 1300 °C). For cokes, the contact angles increase with time and show non-wetting behavior at isothermal temperature 1550 °C while the contact angle for graphite remained more or less the same during wetting. The molten Fe-85wt%Mn was generally non-wetting to coke substrates while graphite which has negligible amount of ash, showed wetting behavior from the beginning. One of the factors causing different behavior of cokes and graphite might be the ash content of cokes.

Effect of ash layer

In complex heterogenous materials such as chars and cokes, several factors can influence the wettability of these carbonaceous sources. These factors include inorganic matter yield and composition in the coke, carbon and sulfur levels in the droplet, carbon structure (microstructure and macrostructure) and formation of phases at the interface due to reactions taking place at the carbon/metal interface.

The sulfur content in the initial metal droplets for all wettability experiments was zero and thus its influence on the wettability of cokes by liquid metal is not investigated in
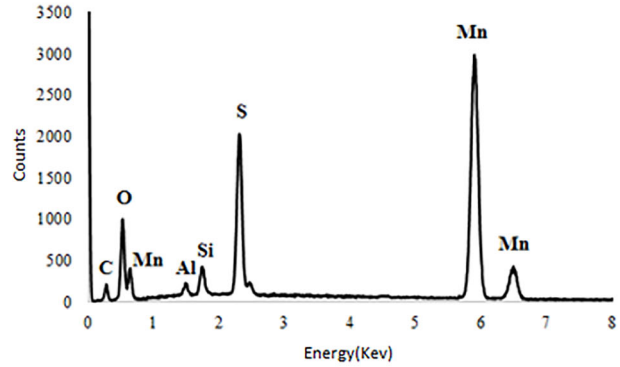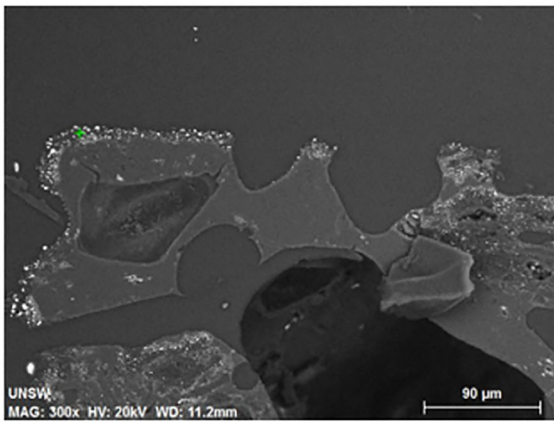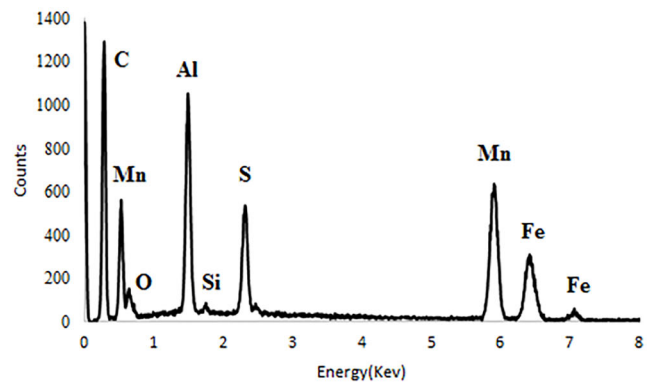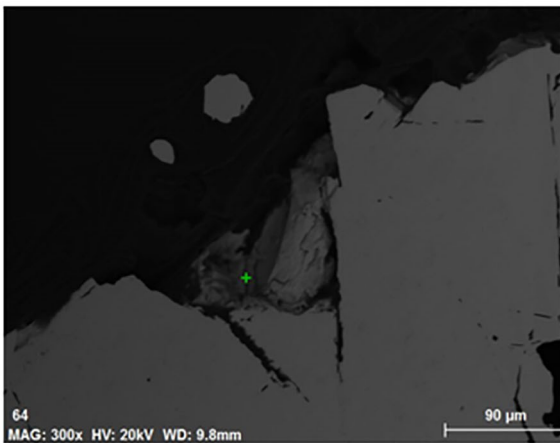
Figure 4. Ash layer including MnS particle in the a) coke side b) metal side of the coke E/metal interface after wetting experiment.

this study. The differences in bulk ash chemistry between the cokes are likely to have some influence on the dynamic changes seen in contact angle during the reaction period. For example, the formation of MnS and alumina and SiC have been observed at the interface as it is shown in Figure 4. The EDS analysis was conducted on a range of coke samples in this study, universal observation was obtained on other locations of sample. Some typical results for coke E were selected and presented in Figure 4. This figure shows that coke E has the highest contact angle and consequently the lowest wettability. Among cokes, coke E has the highest amount of ash and sulfur.

Sulfur and oxygen, which are surface active elements, may decrease the surface tension and consequently decrease the contact angle.[5–8] Presence of S and O was verified by scanning electron microscopy accompanied with energy dispersive spectroscopy of the coke side of the interface as shown in Figure 4a. As shown in Figure 4a, presence of MnS layer which covered the surface can block the surface,[2] was also verified. Figure 4b shows the metal side of the interface and MnS was also detected in this part. As a result, the interfacial products can act as a physical barrier blocking metal and coke contact, thus reducing wettability. Presence of alumina and silica was also verified on the interface and it can be another reason for higher contact angle of

coke E at 1550 °C.[25,26] SiC may also be present at the interface, which could block the reaction surface,[19] as shown in Figure 4.

In addition to ash layer which affects the wettability, there are other factors that may influence the wetting behavior between cokes and metal, such as crystallite size, roughness and porosity of the substrates. A comprehensive microstructure analysis of carbon materials was conducted using XRD and Raman spectroscopy to better understand microstructure characteristic of carbon materials as a function of temperature and how it affects the wettability at high temperature.

Effect of coke microstructure

The XRD profiles of original cokes and cokes annealed at different temperatures are presented in Figure 5. The peaks at 26.6 and 20.8° in original samples were assigned to quartz in the coke ash. They were substantially reduced in annealing above 1250 °C. The shape of the 002 carbon peaks is used as a qualitative indication of the graphitization degree of metallurgical cokes. Coke samples with sharper 002 peaks have a larger crystal size and greater degree of graphitization. The comparison of XRD patterns of coke annealed at
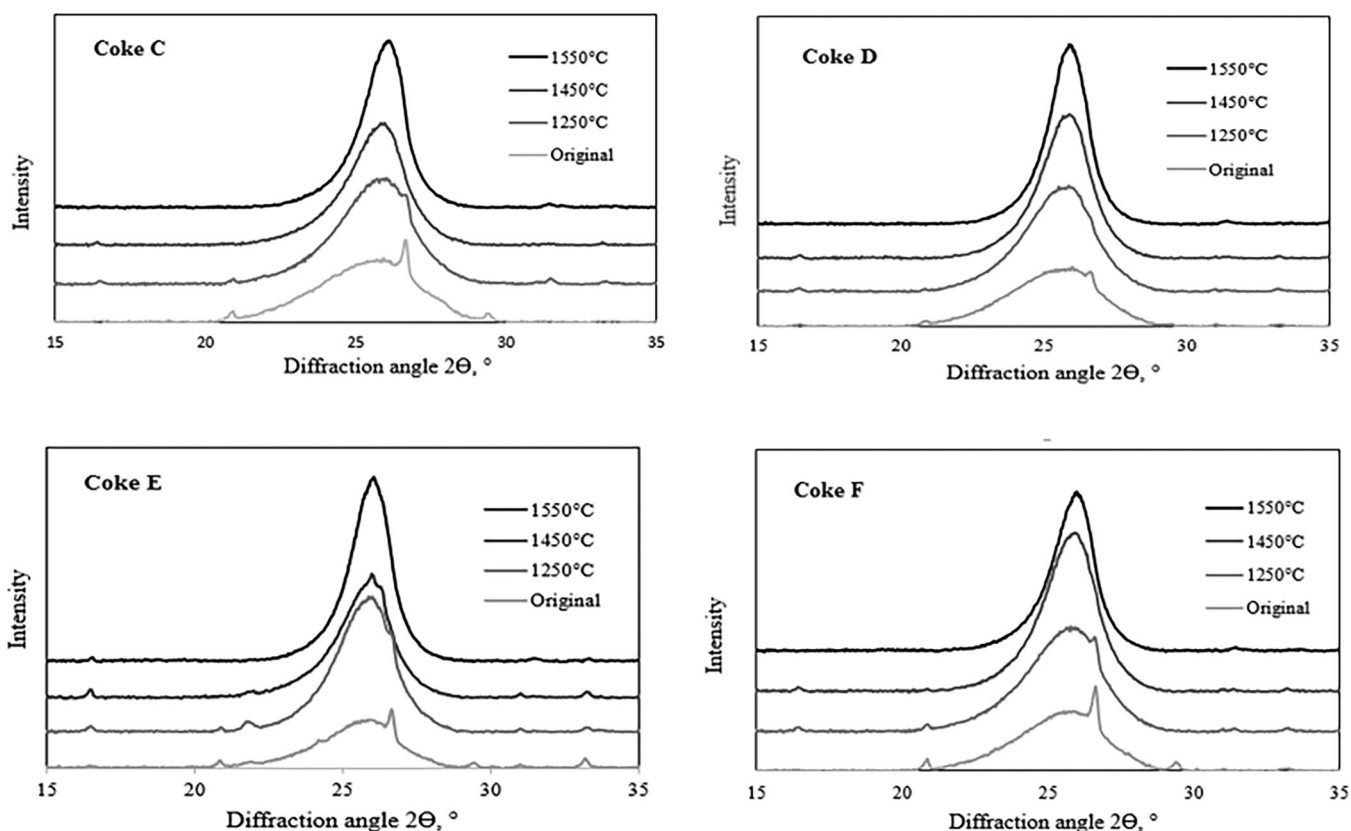
Figure 5. Profiles of 002 carbon peaks in XRD spectra of original cokes C and D, E and F after annealing at different temperatures.
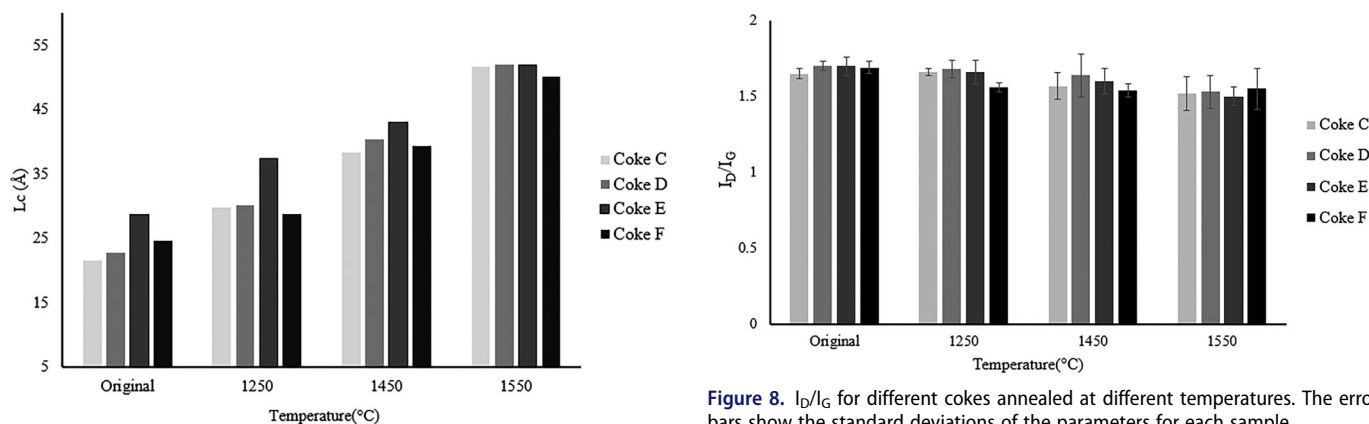

Figure 6. Crystallite size (L_c) of cokes C, D, E and F annealed at different temperatures.

Figure 8. I_D/I_G for different cokes annealed at different temperatures. The error bars show the standard deviations of the parameters for each sample.
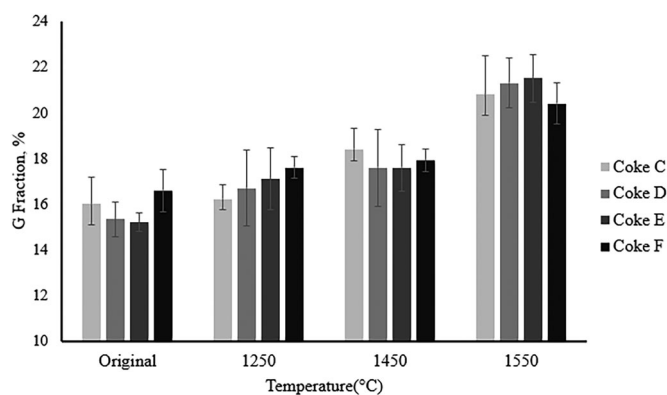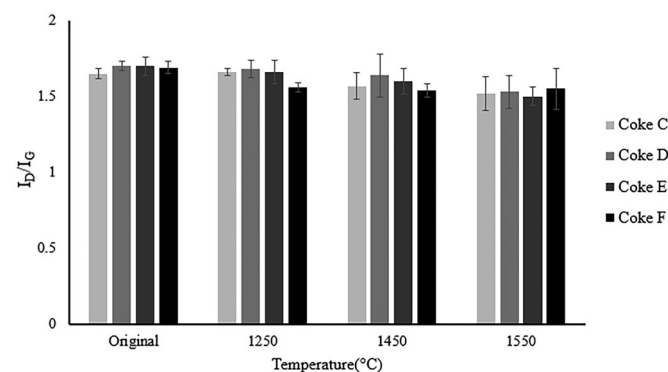

Figure 7. G fraction of different cokes annealed at different temperatures. The error bars show the standard deviations of the parameters for each sample.

different temperatures showed that the 002 carbon peak became sharper with increasing annealing temperature.

The effects of annealing on the carbon crystallite size L_c cokes subjected to different annealing temperature are presented in Figure 6. Coke E had the highest L_c before annealing, it may indicate its higher coking temperature. The crystallite size L_c of all cokes increased significantly with increasing heat treatment temperature and also the difference in L_c among cokes was eliminated by high temperature annealing.

The G fraction of four types of cokes heat treated at different temperatures are presented in Figure 7. G fraction of all cokes increased as annealing temperature increased which indicates that the proportion of graphitic structure
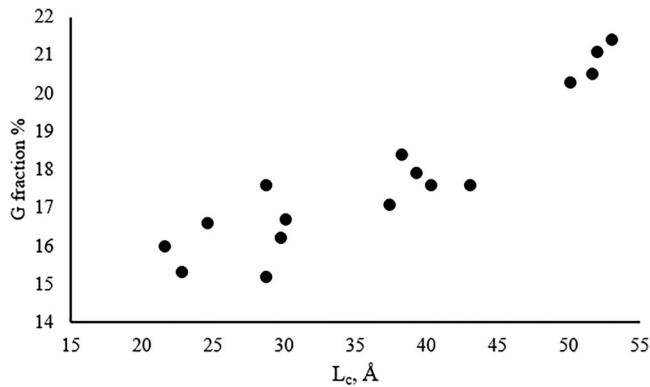
Figure 9. Correlations between Lc and G fraction for cokes subjected to heat treatment at 1250–1550 °C.

Figure 10. Contact angle versus time for different carbon materials.

Table 3. Roughness of the carbon materials.

Carbon material	R$_a$(μm)				Avarage (μm)	Std. deviation (μm)	Std. deviation (%)
	Run 1	Run 2	Run 3	Run 4			
Graphite	9	10	6	7	8	1.58	16
Coke C	65	62	63	–	63	1.29	2
Coke D	71	69	79	–	73	4.32	5.5
Coke E	97	95	98	100	97	1.87	2
Coke F	67	66	68	66	67	0.86	1.2

The standard deviation is given.

Table 4. Porosity determined by pycnometry.

Carbon material	Absolute density (g/cm^3)	Apparent density (g/cm^3)	Porosity%
Graphite	2.05 ± 3%	1.92 ± 2%	6
Coke C	1.81 ± 10%	1.01 ± 15%	44
Coke D	1.85 ± 18%	0.96 ± 11%	48
Coke E	1.93 ± 12%	0.85 ± 12%	55
Coke F	1.87 ± 11%	1.009 ± 9%	46

The standard deviation is given for absolute and apparent density

in cokes increased in the process of thermal annealing. Coke E has the highest G fraction which confirms the results of XRD.

The intensity ratio of the D band to the G band of different cokes with the treatment temperature is shown in Figure 8. General trends can be found that the peak intensity ratio of the D band to the G band decrease slightly for all four types of cokes. The decrease of I_D/I_G band ratios with the increase of the treatment temperature implied that structural defects and imperfections of the carbon crystallites were gradually eliminated during heat treatment.

Figure 9 shows the crystallite size and G fraction of different cokes at 1550 °C. A good correlation can be seen between results from XRD and results from Raman spectroscopy. As Figure 6 shows, the crystallite size of cokes are very close at 1550 °C and L$_c$ of coke E = coke D > coke C > coke F and due to Figure 3, the contact angle of coke E > coke D > coke F > coke C. Thus the different wetting behavior of cokes cannot be explained on the basis of their crystallite size. It was in agreement with findings of Cham[16] who did not see any dependence of wettability between iron and cokes on the coke microstructure and crystallite size.
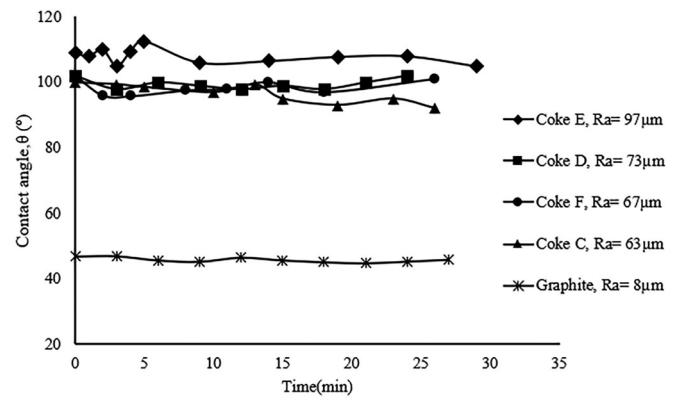
Effect of coke macrostructure

In this study, the uniformity of the surface is supported by the average roughness, R$_a$. The average roughness is the main height as calculated over the entire measured area. Table 3 shows R$_a$ for all carbon materials. The average values are given from three measurements and for some samples from four measurements and show a standard deviation of 11% or less. As Table 3 shows, coke E has the roughest surface and graphite has the smoothest surface.

The porosity of different carbon materials measured by pycnometry is shown in Table 4. Three replicates were done for each sample. As Table 4 shows, graphite has the lowest porosity. Among cokes, coke E has the highest porosity and coke C has the lowest porosity.

Figure 10 shows the changes in contact angle versus time for different carbon materials with different surface roughness. It can be seen from Figure 10 that coke E with the roughest surface and the highest amount of pores, showed the lowest wettability in compare with other cokes. Cokes C and F showed very similar wetting behavior and the roughness and porosity were also very similar. As a result, as the roughness and porosity of the coke increased, the wettability decreased. This may be due to the reason that liquid metal does not penetrate well the rough surface asperities, and gas molecules can be trapped in the asperity valleys. Thus, the interface between liquid and solid is not continuous and there is an alternation of solid-liquid and gas-liquid interfaces. Although results confirmed the finding of Cassie-Baxter, however both Wenzel and Cassie-Baxter models were simulated only for simple deterministic roughness structures (less than 7 μm),[27,28] thus it is difficult to say results of this study follow each of the models.

Figure 11 shows three-dimensional topographic map of different cokes and graphite. Figure 11a shows that the graphite surface is smooth and different with cokes surfaces which have lots of pores.

Conclusion

All cokes showed non-wetting behavior with Fe-85wt%Mn after 30 minutes of contact at 1550 °C. The significance of the formed interfacial products containing MnS on the
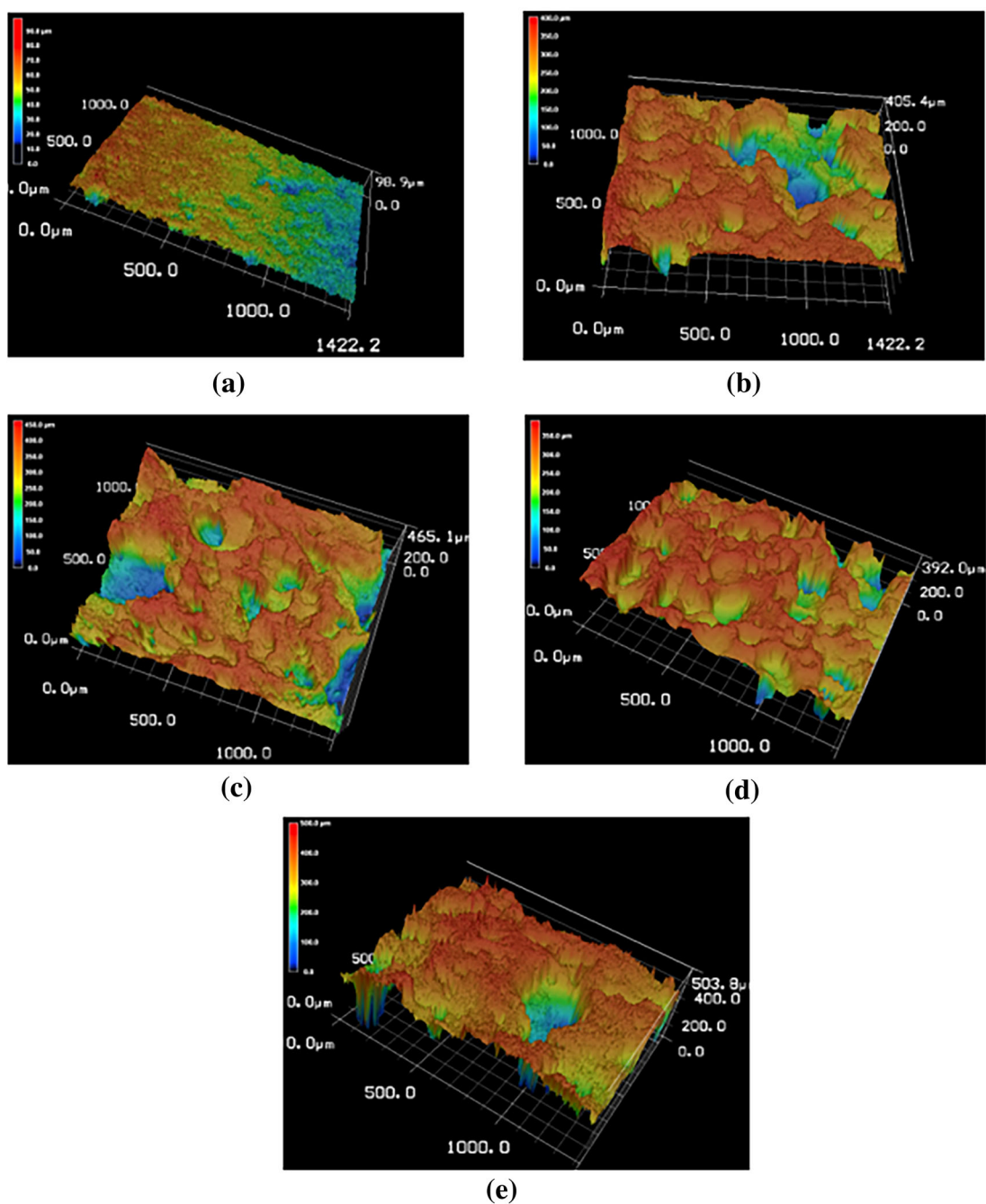
Figure 11. Three-dimensional topographic map of (a) graphite, (b) coke C, (c) coke D, (d) coke E, and (e) coke F at the same magnification.

wetting behavior with metal can be inferred from the observation of graphite behavior. As a result, the interfacial products can act as a physical barrier blocking metal/coke contact and thus reducing the wettability.

In the process of heat treatment, the microstructure of the metallurgical cokes transformed toward a graphite-like structure. Crystallite size increased with increasing temperature. In Raman spectra, which confirmed the XRD results, the G fraction increased with increasing temperature and ratio of D band to G band intensity decreased which indicated the more ordered structure in higher temperature. No significant dependence of wettability on carbon microstructure was seen.

With increasing roughness and porosity of cokes, wettability with Fe-85wt%Mn decreased and the reason was

determined to be due to that liquid metal does not penetrate well the rough surface asperities, and gas molecules can be trapped in the asperity valleys.

ORCID

Hamideh Kaffash 🔟 http://orcid.org/0000-0003-3996-5638

References

[1] Safarian, J. Kinteics and Mechanisms of Reduction of MnO-Containing Silicate Slags by Selected Forms of Carbonaceous Materials. Ph.D Dissertation, Norwegian University of Science and Technology, Trondheim, Norway, **2007**.

[2] Wu, C.; Sahajwalla, V. Dissolution Rates of Coals and Graphite in Fe-C-S in Direct Ironmaking: Influence of Melt Carbon and

Sulfur on Carbon Dissolution. *Metall. Mater. Trans. B* **2000**, *31B*, 243–251. DOI: 10.1007/s11663-000-0043-x.

[3] Wu, C.; Wiblen, R.; Sahajwalla, V. Influence of Ash on Mass Transfer and Interfacial Reaction between Natural Graphite and Liquid Iron. *Metall. Mater. Trans. B* **2000**, *31B*, 1099–1104. DOI: 10.1007/s11663-000-0085-0.

[4] Wu, C.; Sahajwalla, V. Influence of Melt Carbon and Sulfur on the Wetting of Solid Graphite by Fe-C-S Melts. *Metall. Mater. Trans. B* **1998**, *29B*, 471–477. DOI: 10.1007/s11663-998-0126-7.

[5] Rahman, M. M. Fundamental Investigation of Slag/Carbon Interactions in Electric Arc Furnace Steelma-King Process. Ph.D Dissertation, University of New South Wales, Sydney, Australia, **2010**.

[6] Chung, Y.; Cramb, A. W. Dynamic and Equilibrium Interfacial Phenomena in Liquid Steel–Slag Systems. *Metall. Mater. Trans. B* **2000**, *31B*, 957–971. DOI: 10.1007/s11663-000-0072-5.

[7] Keene, B. J. Review of Data for the Surface Tension of Iron and Its Binary Alloys. *Int. Mater. Rev.* **1988**, *33*, 1–37. DOI: 10.1179/imr.1988.33.1.1.

[8] Nakashima, K.; Mori, K. Interfacial Properties of Liquid Iron Alloys and Liquid Slags Relating to Iron-and Steel-Making Processes. *ISIJ Int.* **1992**, *32*, 11–18. DOI: 10.2355/isijinternational.32.11.

[9] Lu, L.; Sahajwalla, V.; Kong, C.; Harris, D. Quantitative X-Ray Diffraction Analysis and Its Application to Various Coals. *Carbon* **2001**, *39*, 1821–1833. DOI: 10.1016/S0008-6223(00)00318-3.

[10] Xing, X.; Zhang, G.; Rogers, H.; Zulli, P.; Ostrovski, O. Effects of Annealing on Microstructure and Microstrength of Metallurgical Coke. *Metall. Mater. Trans. B* **2014**, *45B*, 106–112. DOI: 10.1007/s11663-013-0002-y.

[11] Kawakami, M.; Kanba, H.; Sato, K.; Takenaka, S.; Gupta, S.; Chandratilleke, R.; Sahajwalla, V. Characterization of Thermal Annealing Effects on the Evolution of Coke Carbon Structure Using Raman Spectroscopy and x-Ray Diffraction. *ISIJ Int.* **2006**, *46*, 1165–1170. DOI: 10.2355/isijinternational.46.1165.

[12] Kawakami, M.; Karato, T.; Takenaka, T.; Yokoyama, S. Structure Analysis of Coke, Wood Charcoal and Bamboo Charcoal by Raman Spectroscopy and Their Reaction Rate with CO_2. *ISIJ Int.* **2005**, *45*, 1027–1034. DOI: 10.2355/isijinternational.45.1027.

[13] Guedes, A.; Valentim, B.; Prieto, A. C.; Rodrigues, S.; Noronha, F. Micro-Raman Spectroscopy of Collotelinite, Fusinite and Macrinite. *Int. J. Coal Geol.* **2010**, *83*, 415–422. DOI: 10.1016/j.coal.2010.06.002.

[14] Deng, J.; Zhang, J.; Jiao, K. Dissolution Mechanism of Carbon Brick into Molten Iron. *ISIJ Int.* **2018**, *58*, 815–822. DOI: 10.2355/isijinternational.ISIJINT-2017-659.

[15] Mourao, M.; Krishna Murthy, G.; Elliott, J. Experimental Investigation of Dissolution Rates of Carbonaceous Materials in Liquid Iron-Carbon Melts. *Metall. Mater. Trans. B* **1993**, *24B*, 629–637. DOI: 10.1007/BF02673178.

[16] Cham, S. T. Investigating Factors That Influence Carbon Dissolution from Coke into Molten Iron. Ph.D Dissertation, University of New South Wales, Sydney, Australia, **2007**.

[17] Bico, J.; Thiele, U.; Quere, D. Wetting of Textured Surfaces. *Colloids Surf. A* **2002**, *206*, 41–46. DOI: 10.1016/S0927-7757(02)00061-4.

[18] Bormashenko, E.; Pogreb, R.; Whyman, G.; Erlich, M. Cassie-Wenzel Wetting Transition in Vibrating Drops Deposited on Rough Surfaces: Is the Dynamic Cassie-Wenzel Wetting Transition a 2D or 1D Affair? *Langmuir* **2007**, *23*, 6501–6503. DOI: 10.1021/la700935x.

[19] Wenzel, R. N. Resistance of Solid Surfaces to Wetting by Water. *Ind. Eng. Chem.* **1936**, *28*, 988–994. DOI: 10.1021/ie50320a024.

[20] Cassie, A. B. D.; Baxter, S. Wettability of Porous Surfaces. *Trans. Faraday Soc.* **1944**, *40*, 546–551. DOI: 10.1039/tf9444000546.

[21] Koishi, T.; Yasuoka, K.; Fujikawa, S.; Ebisuzaki, T.; Zeng, X. C. Coexistence and Transition between Cassie and Wenzel State on Pillared Hydrophobic Surface. *Proc. Natl. Acad. Sci. USA* **2009**, *106*, 8435–8440. DOI: 10.1073/pnas.0902027106.

[22] Ciftja, A. Solar Silicon Refining; Inclusions, Settling, Filtration, Wetting. Ph.D Dissertation, Norwegian University of Science and Technology, Trondheim, Norway, **2009**.

[23] Lee, Y. E. Ferroalloys: Production and Use in Steel-Making. *Encycl. Mater. Sci. Technol.* **2001**, *1*, 3039–3043. DOI: 10.1016/B0-08-043152-6/00544-1.

[24] Bhardwaj, B. P. *The Complete Book on Ferroallloys*; Niir Project Consultancy Services: Delhi, India, **2014**.

[25] Zhao, L.; Sahajwalla, V. Interfacial Phenomena during Wetting of Graphite/Alumina Mixtures by Liquid Iron. *ISIJ Int.* **2003**, *43*, 1–6. DOI: 10.2355/isijinternational.43.1.

[26] Ohno, K. I.; Miyake, T.; Yano, S.; Nguyen, C. C.; Maeda, T.; Kunitomo, K. Effect of Carbon Dissolution Reaction on Wetting Behavior between Liquid Iron and Carbonaceous Material. *ISIJ Int.* **2015**, *55*, 1252–1258. DOI: 10.2355/isijinternational.55.1252.

[27] Coriand, L. Roughness, Wetting, and Optical Properties of Functional Surfaces. Ph.D Dissertation, Friedrich Schiller University Jena, Jena, Germany, **2014**.

[28] He, L.; Farson, D. F.; Rokhlin, S. Wettability Modification of Electrospun Poly(ε-Caprolactone) Fiber by Femtosecond Laser Irradiation. *J. Laser Appl.* **2013**, *25*, 1–8.